ISSN 1063-7710, Acoustical Physics, 2015, Vol. 61, No. 3, pp. 301–307. © Pleiades Publishing, Ltd., 2015.
Original Russian Text © P.B. Rosnitskiy, P.V. Yuldashev, V.A. Khokhlova, 2015, published in Akusticheskii Zhurnal, 2015, Vol. 61, No. 3, pp. 325–332.

NONLINEAR ACOUSTICS

Effect of the Angular Aperture of Medical Ultrasound Transducers on the Parameters of Nonlinear Ultrasound Field with Shocks at the Focus

P. B. Rosnitskiy, P. V. Yuldashev, and V. A. Khokhlova
Moscow State University, Physics Faculty, Moscow, 119991 Russia
e-mail: pavrosni@yandex.ru
Received October 22, 2014

Abstract—Certain modern applications of high-intensity focused ultrasound (HIFU) in medicine use the nonlinear effect of shock front formation in the focal waveform. However, an important problem remains unsolved: determination of transducer parameters that provide the given pressure levels of the shock wave field at the focus required for a specific application. In this paper, simulations based on the Khokhlov–Zabolotskaya equation are performed to test and confirm the hypothesis that angular aperture of the transducer is the main parameter that determines the characteristic amplitude of the shock front and corresponding values for the peak positive and negative pressures at the focus. A criterion for formation of a developed shock in the acoustic waveform, as well as a method for determining its amplitude is proposed. Quantitative dependences of the amplitude of the developed shock and the peak pressures in the wave profile on the angular aperture of the transducer are calculated. The effects of saturation and the range of changes of the shock waveform parameters at the focus are analyzed for a typical HIFU transducer.

Keywords: nonlinear waves, focusing, diffraction, shock front, medical acoustics, ultrasound surgery, histotripsy
DOI: 10.1134/S1063771015030148

INTRODUCTION

During last ten years, new medical applications have rapidly developed for high-intensity focused ultrasound (HIFU). One such application is noninvasive ultrasound surgery, in which a high-intensity beam is focused through the skin to induce rapid localized heating of tissues within the human body [1]. This approach has been already used to destroy tumors in various organs: uterus, prostate, liver, kidneys, and thyroid [2]. Research continues on the possibility of applying HIFU to stop internal bleeding, for targeted drug delivery, thrombolysis, treating arrhythmia, stimulating the growth of micro vessels after heart attack, and others [1–3]. Recently, the first successful surgeries were conducted on brain for treating essential tremor and destroying metastatic brain tumors via ultrasound irradiation through the skull [4].

The typical time necessary to destroy tumors of several cubic centimeters in volume in MRI-controlled HIFU clinical systems is about several hours [5]. To accelerate the treatment, ultrasound-controlled high-power systems are used, for which the intensity levels at the focus achieve 10–30 kW/cm^2 [6]. When analyzing the operation of such transducers, it is necessary to take into account nonlinear effects and possible formation of shock fronts in the wave profile in the focal region of the transducer. HIFU irradiation protocols that utilize high-amplitude shock fronts attract the attention of researchers, since the efficiency of ultrasound energy absorption at the shocks and the corresponding thermal effect can increase more than tenfold in comparison to a harmonic wave of the same amplitude [3, 7–10].

Recently, two fundamentally novel ultrasound surgical methods were developed based not on thermal, but on mechanical destruction of tissue (histotripsy) [7, 11, 12]. Both methods use a pulsed-periodic irradiation protocol with a duty factor of <1%. One uses microsecond-long pulses that generate a cavitation cloud in the focal region, and the other uses millisecond-long pulses that induce localized boiling of tissue within each pulse. Despite the different physical mechanisms of action, both methods make it possible to mechanically disintegrate tissue into subcellular fragments without a thermal effect of tissue denaturation. Histotripsy has a number of clinical advantages in comparison to thermal action. For example, liquefaction of tissue during histotripsy, in contrast to thermal necrosis, can facilitate easier removal of destroyed tissue debris from the body. Recent preclinical histotripsy trials on hyperplasia of the prostate gland (adenoma) in a dog model have shown that the destroyed tissue was removed through the excretory system over the course of several days [13]. To implement treatments involving histotripsy, extremely high intensities

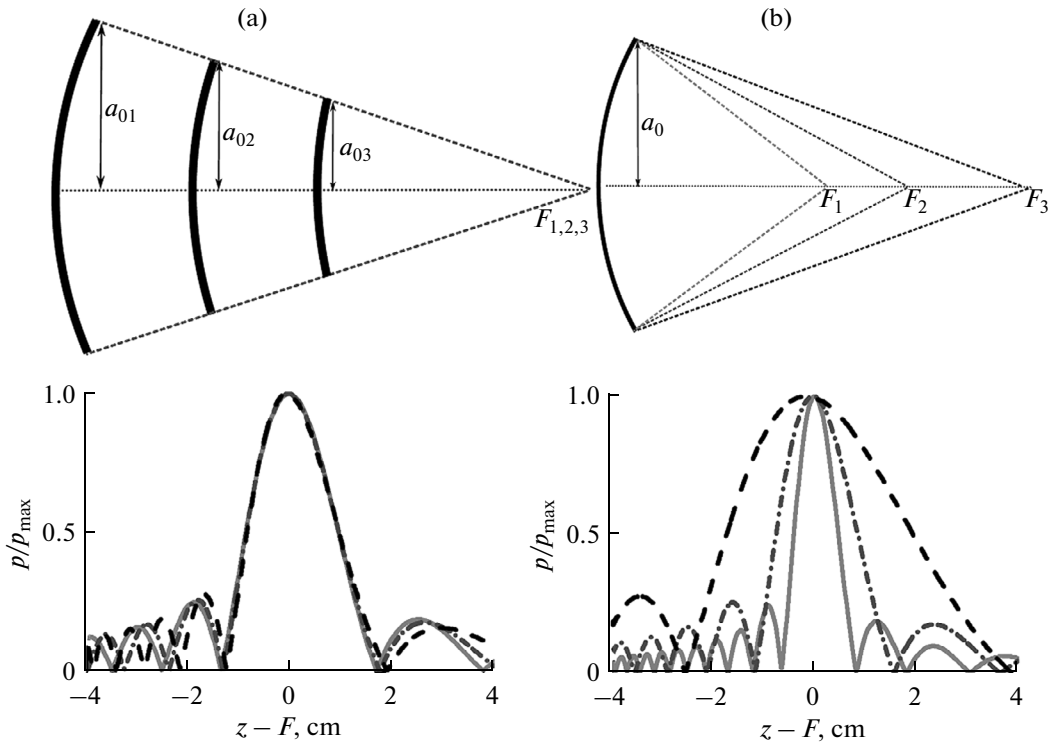

Fig. 1. On-axis pressure amplitude distributions p/p_{max} normalized to their maximum values in linear beams generated by focused transducers (a) with identical and (b) different angular apertures. Here, a_0 is the transducer radius, F is its focal distance, and z is the coordinate along the transducer axis. Examples are given for transducers with 1.5 MHz frequency and (a) $F = 8$, 12, 16 cm; $F_{number} = 1.5$; (b) $F = 8$, 12, 16 cm; $F_{number} = 1$, 1.5, 2.

(>30 kW/cm^2) and in most cases the presence of high-amplitude shock fronts (>60 MPa) at the focus are necessary.

To develop HIFU protocols that utilize shock wave action on tissue, it is necessary to predict the characteristic amplitude of shock fronts and the corresponding peak pressures for a specific transducer or to develop transducers with specific parameters that ensure the desired shock wave field pressure levels. For example, histotripsy requires shocks with an amplitude on the order of 60–120 MPa [7]. On the other hand, for purely thermal ablation methods, the absence of shock fronts is preferable, because formation of shocks changes the predicted heating pattern in tissue and thus requires changes in the irradiation protocol. For applications that use a cavitation effect, the peak negative pressure in the focal waveform is the most important parameter for treatment planning. However, up to date, no approach has been developed for determining transducer parameters that provide the given values of the shock wave field parameters at the focus of HIFU transducers. Such an approach is proposed in this study.

One of the important transducer parameters is its angular aperture φ, the angle at which the diameter of the transducer (or its aperture) is visible from the focus point (Fig. 1). If the transducer is weakly focused, the length of the focal diffraction maximum of the beam is larger than for the strong focusing. The figure shows the pressure amplitude distributions on the axis of linearly focused beams for transducers of different geometry. The distributions are calculated using the Rayleigh integral and are normalized to the corresponding maximum values of the pressure amplitude of the acoustic wave on the beam axis. The focusing strength of ultrasound transducers is usually characterized by the parameter $F_{number} = F/2a_0$ (an analog of f-number in optics), where F is the focal length of the transducer and a_0 is its radius. The parameter F_{number} is related to the angular aperture of the transducer by the simple equation $F_{number} = (2\sin(\varphi/2))^{-1}$. Clearly, for transducers of different diameter but with the same angular aperture, the shape and the length of the focal maximum are very close to each other (Fig. 1a). In the case of transducers with different angular apertures, they differ significantly (Fig. 1b). These estimates are valid for transducers whose dimensions strongly exceed the wavelength ($ka_0 \gg 1$, k is the wavenumber). This condition is almost always fulfilled for medical transducers used for HIFU applications.

Since nonlinear effects accumulate with distance and are most strongly pronounced in the high-amplitude focal region of the beam, shock fronts for weakly focused beams will form at lower pressure levels at the focus than for strongly focused beams. With further

increase in pressure at the beam focus, the amplitude of the shock will increase, but then will saturate quite rapidly [8, 14]. Thus, by regulating the focusing angle, it is possible to achieve the given characteristic values of the shock amplitude in the focal waveform. The goal of this study was to determine the dependence of the main parameters characterizing the developed shock front at the focus of a transducer on its angular aperture and to validate the hypothesis that the type of shock front is independent of other transducer parameters.

THEORETICAL MODEL

Let us consider an ultrasound beam generated from a single element focused transducer of a spherical segment shape. Such a choice is both suitable for numerical analysis due to the radial field symmetry, and is sufficiently general. To simulate numerically the nonlinear fields generated by such transducers, we will use the parabolic Khokhlov–Zabolotskaya–Kuznetsov (KZK) equation with weak viscosity [8–10, 15, 16]. The boundary condition to the KZK equation is specified on a plane: a spherical segment with a uniform distribution of the amplitude of vibrational velocity and a constant phase is replaced by a plane circle with constant pressure amplitude; focusing is done by changing the phase according to a parabolic law as a function of the radial coordinate. Note that with special modifications to the boundary condition, the KZK method yields highly accurate results even when describing fields of strongly focused transducers [17–19].

For medical applications, of ultimate interest is the prediction and control of the shock wave field parameters not in water, but in absorbing biological tissue. Recent studies [20] proposed a derating method for recalculating data obtained in water at the beam focus to biological tissue for nonlinear HIFU fields. It was shown that in tissue, the shock front amplitude and peak pressures will be the same as in water, only for a larger initial transducer power, which compensates linear losses of the beam energy in the prefocal region. Thus, the results obtained in simulation of the KZK equation in water also give necessary information on the field parameter values in tissue [10, 12].

Let us write the KZK equation and boundary condition in parabolic approximation for a circular transducer with a uniform pressure amplitude distribution in dimensionless form [8]:

$$\frac{\partial}{\partial\theta}\left(\frac{\partial P}{\partial\sigma} - NP\frac{\partial P}{\partial\theta} - A\frac{\partial^2 P}{\partial\theta^2}\right) = \frac{1}{4G}\Delta_\perp P,$$
$$P(\sigma = 0, R, \theta) = \begin{cases}\sin\left(\theta + GR^2\right), & R \le 1\\ 0, & R > 1.\end{cases} \quad (1)$$

Here, $P = p/p_0$ is the acoustic pressure normalized to the pressure amplitude at the transducer p_0, $\theta = \omega_0(t - z/c_0)$ is the dimensionless time in a moving coordinate system; $\omega_0 = 2\pi f_0$, f_0 is the transducer frequency; c_0 is the sound velocity; $\sigma = z/F$ is the coordinate along the beam axis normalized to focal length F; $R = r/a_0$ is the radial coordinate normalized to the transducer radius a_0; $N = 2\pi F f_0 \varepsilon p_0 / c_0^3 \rho_0$ is the dimensionless nonlinear parameter; ε is the nonlinearity of the medium; ρ_0 is the density of the medium; $G = \pi f_0 a_0^2 / c_0 F$ is the diffraction parameter (the linear coefficient of pressure amplification with respect to the pressure amplitude on the surface of the transducer); and A is the absorption parameter.

The value of the absorption coefficient when focusing in water is considered to be very small, $A \ll 1$, and it affects only the fine structure of shock fronts that are developing in the wave profile. Thus, the nonlinear ultrasound field generated by a focused transducer in such a medium will depend on only two parameters: N and G [8]. The parameter N characterizes the pressure magnitude at the transducer, and the diffraction parameter G is a combination of dimensionless parameters ka_0 and F_{number} : $G = ka_0/4F_{\text{number}}$.

To reveal the dependence of the parameters of the focal waveforms with shock fronts on the transducer parameters, the dimensionless KZK equation was solved for different values of parameters G and N. The diffraction parameter changed within the range of $10 \le G \le 75$ with the step of $\Delta G = 5$. For each value of parameter G, 75 values of the nonlinear parameter within the range $0 \le N \le 1.5$ were considered. The step in changing N was variable: $\Delta N = 0.01$ within the range $0 < N < 0.5$, where rapid changes in the spatial structure of the field and focal waveform occur with increasing N, and $\Delta N = 0.04$ for $0.5 < N < 1.5$, where changes are slower (see below). The initial absorption value was $A = 0.0025$, and it automatically increased during shock formation, to keep six to eight time grid nodes at the shock front. As a result of numerical simulations, dimensionless waveforms at the focus $P_F(\theta)$ (for $\sigma = 1$) were obtained for all considered values of G and N. These waveforms were used to study the dependence of the shock amplitude and peak pressure values on the transducer parameters.

As an example, let us consider the evolution of the wave profile at the focus with increasing initial pressure amplitude at the transducer with a frequency of 1 MHz, $F = 10$ cm, $a_0 = 5.4$ cm; in this case, $G = 60$ (Fig. 2a). With increasing value of parameter N, the dimensionless wave profile at the focus $P_F(\theta) = p_F/p_0$ becomes steeper (curve *1*) and a shock front forms; its amplitude first increases (curve *2*), then starts to decrease (curve *3*) due to strong absorption of the wave energy at the shock front in the prefocal region. In order to introduce the concept of the shock amplitude characteristic for this transducer, we consider that a fully developed shock corresponds to the situation when the shock amplitude in the dimensionless profile reaches the maximum value.

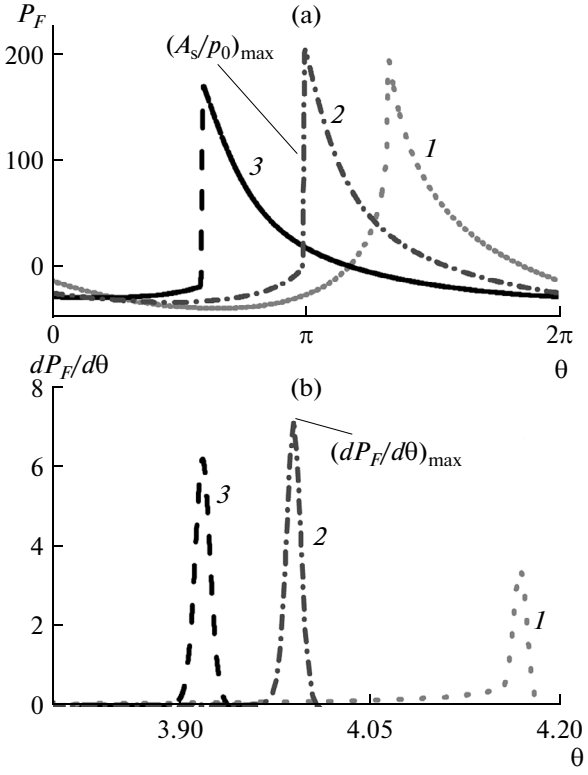

Fig. 2. (a) Dimensionless waveforms $P_F = p_F/p_0$ at the focus for $G = 60$, that correspond to different values of nonlinear parameter N, and (b) their time derivatives $dP_F/d\theta$. The dotted line *1* ($N = 0.17$) corresponds to the onset of shock formation; the dash-dotted line *2* ($N = 0.27$) corresponds to the waveform with maximum shock amplitude $(A_s/p_0)_{max}$ and maximum peak value of the derivative $(dP_F/d\theta)_{max}$; the dashed line *3* ($N = 0.37$) corresponds to the onset of the saturation effect.

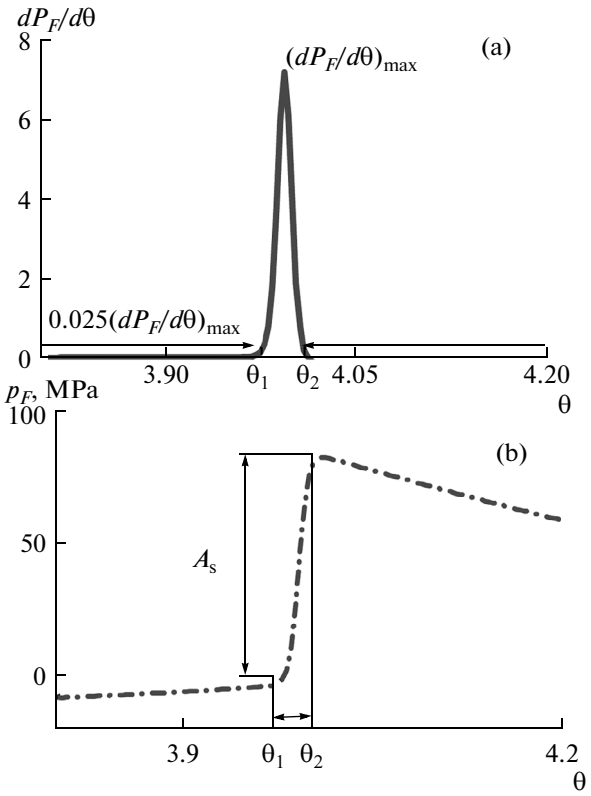

Fig. 3. Determination of the shock amplitude A_s in a wave profile. (a) Time points θ_1 and θ_2 are shock boundaries determined at the threshold level of 0.025 from the maximum derivative $dP_F/d\theta$; (b) dimensional waveform with the shock front determined from this level. The plots are calculated for a transducer with the following parameters: $f_0 = 1$ MHz, $F = 10$ cm, $a_0 = 5.4$ cm, $p_0 = 0.41$ MPa ($N = 0.27$, $G = 60$).

Let us determine the dimensionless wave profile $P_F(\theta)$ with the maximum shock amplitude when the time derivative $\dot{P}_F = dP_F/d\theta$ of the profile reaches the maximum value (Fig. 2b). Clearly, the formation of a shock is accompanied by the appearance of a peak in the plot of the time dependence of the derivative. The Godunov's shock-capturing scheme used here in the numerical model ensures the same number of points at the shock front, i.e. its constant width:

$$\Delta\theta = \theta_2 - \theta_1 = \text{const}, \qquad (2)$$

where θ_1 and θ_2 are the time instants that correspond to the boundaries of the shock (Fig. 3). Thus, the derivative of the dimensionless waveform, which can be approximated by a straight line in the shock region $\theta_1 < \theta < \theta_2$, according to (2), will have the form

$$\dot{P}_F \approx \frac{(A_s/p_0)}{\Delta\theta} = \text{const}(A_s/p_0), \qquad (3)$$

where $A_s/p_0 = P_F(\theta_2) - P_F(\theta_1)$ is the shock amplitude in the dimensionless wave profile and A_s is the shock amplitude in the dimensional wave profile. Hence one can see that the maximum value of the derivative—the highest peak in the derivative plot (Fig. 2b)—will correspond to the dimensionless profile with the maximum shock amplitude.

After determining the focal waveform with a fully developed shock in each series of calculations with constant G and increasing N, the problem is how to determine its amplitude. Let us define the shock boundaries θ_1 and θ_2 at some given threshold level s of the peak of its time derivative with respect to its maximum (Fig. 3a). With a change in parameter s, there is a change in the time interval between θ_1 and θ_2 and, correspondingly, in the shock amplitude (Fig. 3b):

$$A_s/p_0 = P_F(\theta_1) - P_F(\theta_2). \qquad (4)$$

Since the shock amplitude is commonly used in HIFU studies to estimate the heating induced by ultrasound waves in tissue [8–10, 12], the parameter s can be introduced as follows. Let us clarify such a choice using an example of transducers with an operating frequency of $f_0 = 1$ MHz, a focal length of $F = 10$ cm, a variable radius a_0 corresponding to a change in the dif-

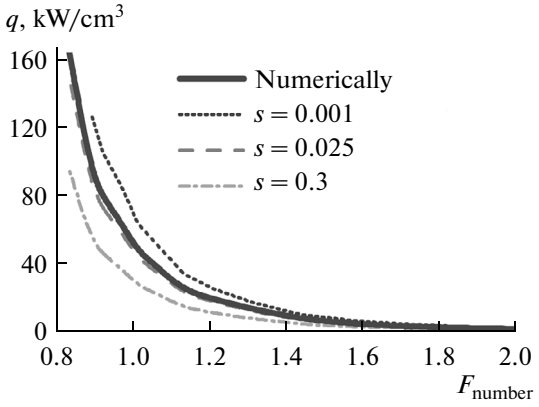

Fig. 4. Dependencies of heat emission q at the shock at the focus on the transducer angular aperture (numerically—calculated numerically; $s = 0.001$, 0.025, 0.3—calculated from the shock amplitude using corresponding levels s). The plots are calculated for a transducer with the following parameters: $f_0 = 1$ MHz, $F = 10$ cm, $a_0 = 2.2$–6 cm, $G = 10$–75.

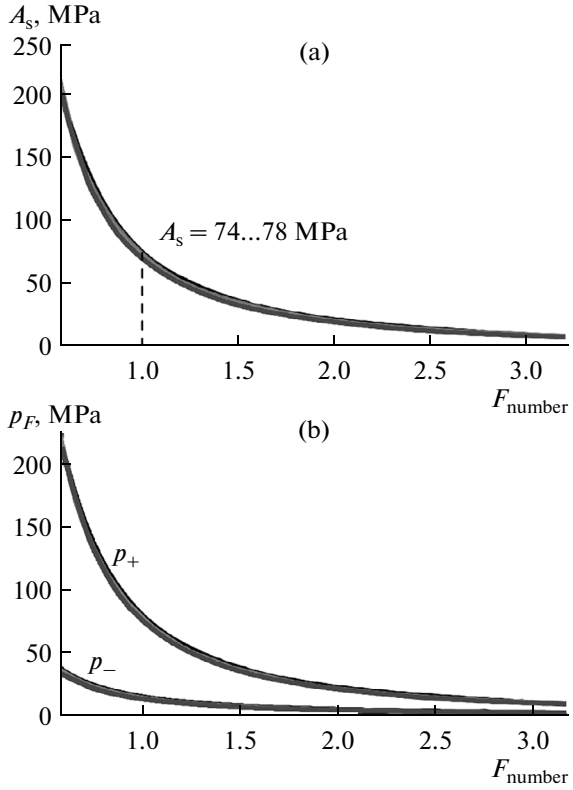

Fig. 5. Dependencies of the parameters of the focal waveform with a fully developed shock (A_s, p_+, and p_-) on angular aperture of transducer for different values of parameter $ka_0 = 126$, 147, 168, 188. For angular aperture $F_{number} = 1$, the shock amplitude values lie within a range of $A_s = 74$–78 MPa.

fraction parameter in the range $10 \le G \le 75$, and amplitude p_0 on the transducer surface corresponding to a change in the nonlinear parameter for each fixed G in the range $0 \le N \le 1.5$. Let us calculate the heat deposition q caused by wave energy absorption at the focus by two methods: using the weak shock theory and the shock amplitude [9, 10]:

$$q = \frac{\varepsilon f_0 A_s^3}{6c_0^4\rho_0^2}, \tag{5}$$

and by direct numerical modeling [8, 10]. Figure 4 shows the dependence of heat deposition versus angular aperture F_{number} calculated either numerically or from the shock amplitude determined at different levels s: $s = 0.001$, 0.025, 0.3. As one can see, for $s = 0.3$, the values of the shock amplitude and heat deposition are underestimated in comparison to direct calculations; for $s = 0.001$, they are overestimated. For $s = 0.025$, the best correspondence of the analytic estimate (5) and direct numerical simulations was observed. This threshold value was used further in this study when determining the shock amplitude in the wave profile.

Using the proposed method, the values of nonlinearity $N_{dev}(G)$ were obtained, which correspond to fully developed shocks in focal waveforms of the beams with different values of diffraction parameter G, and the amplitudes of these shocks A_s/p_0 were determined in the form of some function $\psi(G)$:

$$A_s/p_0 = \psi(G). \tag{6}$$

Knowing function ψ, one can easily show that amplitude A_s of a fully developed shock at the focus is determined by two dimensionless transducer parameters: its aperture measured in ultrasound wavelengths ka_0, and angular aperture determined by the F_{number}. Indeed, from the definition of parameters N, G, and F_{number}, it follows that

$$N = \frac{F 2\pi f_0 \varepsilon p_0}{c_0^3\rho_0} \Rightarrow p_0 = \frac{c_0^2\rho_0 N}{2\varepsilon F_{number} ka_0}, \tag{7}$$

$$G = \frac{\pi f_0 a_0^2}{c_0 F} = \frac{ka_0}{4F_{number}}. \tag{8}$$

Then, for the shock amplitude A_s, using (6), we can write

$$A_s = (A_s/p_0)\,p_0 = (A_s/p_0)\frac{c_0^2\rho_0 N}{2\varepsilon F_{number} ka_0}. \tag{9}$$

Substituting the expression for A_s/p_0 (6) and expression (8) for parameter G in (9), we obtain the dependence of the amplitude of the developed shock A_s for different values of the transducer parameters ka_0 and F_{number}:

$$A_s = \psi\left(\frac{1}{4}\frac{ka_0}{F_{number}}\right)\frac{c_0^2\rho_0}{2\varepsilon F_{number} ka_0} N_{dev}\left(\frac{1}{4}\frac{ka_0}{F_{number}}\right). \tag{10}$$

Other parameters of the shock wave profile are determined in a similar way: the peak positive pressure p_+ (maximum pressure in the focal waveform)

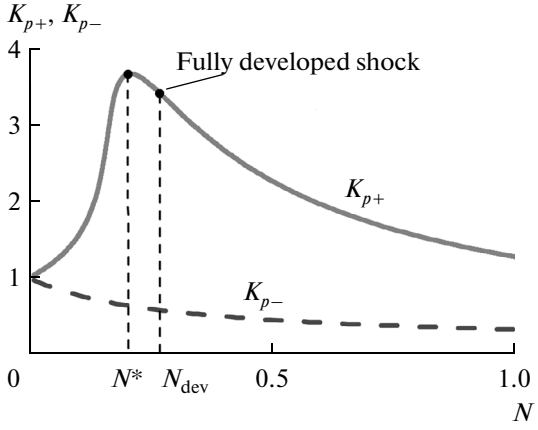

Fig. 6. Dependence of correction index to concentration coefficient for peak positive K_{p_+} and negative K_{p_-} pressures on dimensionless nonlinear parameter N. $N^* = 0.2$ is the nonlinear parameter corresponding to the maximum value K_{p_+}, N_{dev} is fully developed shock. For the example, the following transducer parameters were used: $f_0 = 1$ MHz, $F = 10$ cm, $a_0 = 5.4$ cm, $G = 60$.

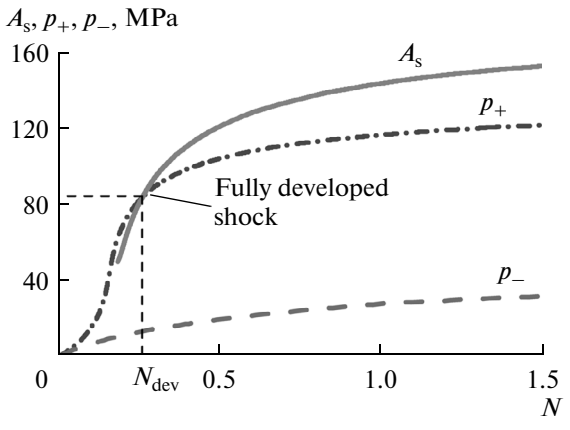

Fig. 7. Saturation curves for the shock amplitude A_s, peak positive p_+, and peak negative p_- pressures. The plots are calculated for a transducer with the following parameters: $f_0 = 1$ MHz, $F = 10$ cm, $a_0 = 5.4$ cm, $G = 60$.

and the peak negative pressure p_- (absolute value of minimum pressure in the focal waveform).

RESULTS

Figure 5 shows the dependence of the shock amplitude A_s and the peak pressures p_+ and p_- on the angular aperture F_{number} for different values of parameter ka_0 = 126, 147, 168, 188 that are typical for HIFU, e.g., transducers with 1 MHz frequency and radii of a_0 = 3, 3.5, 4, 4.5 cm. Clearly, the curves obtained for different ka_0 values are virtually indistinguishable. Since the parameters of waveforms with a fully developed shock depend only on the two parameters, ka_0 and F_{number} (10), angular aperture F_{number} is indeed the main parameter that determines the parameters of the wave profile with a developed shock at the focus. With increasing F_{number}, i.e., with decreasing focusing angle, the shock amplitude decreases, which fully corresponds to the qualitative ideas given in the Introduction. Note especially the case of $F_{number} = 1$ and corresponding shock amplitude of about 80 MPa (Fig. 3b). This value is characteristic for transducers and focal waveforms used in histotripsy [7]. The plots in Fig. 5 make it possible to determine the parameters of a transducer that would generate focal waveforms with given values of the shock amplitude and peak pressures. The obtained quantitative data can be used for developing transducers for various specific HIFU applications.

Now let us consider how the value of $N_{dev}(G)$ is related to previously known changes in the HIFU beam parameters, which manifest themselves with increase of nonlinear effects. One of the most important characteristics of focusing systems is the concentration coefficient, i.e., the ratio of the value of a certain acoustic parameter of the field at the focus to the corresponding value at the transducer surface. In case of a linear harmonic wave focusing, in the KZK model, the concentration coefficient for the pressure amplitude is equal to the diffraction parameter $G = \pi f_0 a_0^2/c_0 F = ka_0/4F_{number}$. For nonlinear focusing, it is convenient to consider correction indices to the concentration coefficients of the field at the focus: $K = G_{nonlin}/G_{lin}$ [8]. Here G_{lin} and G_{nonlin} are the linear and nonlinear concentration coefficients for different waveform parameters. For the peak positive and negative pressures, the correction indices will obviously be $K_{p_\pm} = p_\pm/p_0 G$. Figure 6 shows an example of the dependence of correction indices K_{p_+} and K_{p_-} for the peak pressures on dimensionless nonlinear parameter N for transducer operating at 1 MHz frequency, $F = 10$ cm, $a_0 = 5.4$ cm, and $G = 60$. Clearly, the nonlinearity parameter, which corresponds to a fully developed shock $N_{dev}(G = 60) = 0.27$, is 35% higher than the parameter corresponding to the maximum of the correction index K_{p_+} for the peak positive pressure $N^* = 0.2$, for which the shock front at the focus only begins to form [8]. Figure 7 shows the dependencies of the shock amplitude A_s, the peak positive p_+, and peak negative p_- pressures on the pressure amplitude at the transducer (parameter N). It is interesting that for the profile with fully developed shock, $N_{dev} = 0.27$, the peak positive pressure p_+ and the shock amplitude A_s are equal; i.e., in practice, such a profile can be determined when the lower pressure value of the shock hits a zero level. It is also clear that the point N_{dev} is close to the inflection point on the saturation curve A_p; i.e., it encloses an area of the rapid growth of the shock amplitude. With further increase in N, saturation of

the focal waveform parameters occurs. For example, with a twofold increase in amplitude ($N = 2N_{dev} = 0.54$), the shock amplitude A_s increases by only 47% and reaches the value of 125 MPa; the peak positive pressure p_+ increases by 25% (106 MPa); and the peak negative pressure p_-, by 50% (21 MPa). For a threefold increase ($N = 3N_{dev} = 0.81$), the corresponding increase is: A_s—62% (138 MPa); p_+ —34% (114 MPa); p_- —86% (26 MPa). For $N = 4N_{dev} = 1.08$: A_s—72% (146 MPa), p_+ —39% (118 MPa), p_- —107% (29 MPa). Note that a fourfold increase in amplitude at the transducer surface with respect to N_{dev} can be achieved in practice only for specially developed devices [21].

CONCLUSIONS

This paper showed that parameters of the shock wave field at the focus of the ultrasound transducer are mainly determined by its angular aperture. Of course, it is also necessary to ensure sufficient power to achieve the shock wave formation regime. Based on numerical simulations of the KZK equation, a method was developed to solve the inverse problem of determining the angular aperture of a transducer to generate a shock front with the given amplitude and the corresponding peak pressures in the focal waveform. A criterion was proposed for determining a fully developed shock, as well as a method for determining its amplitude by matching the heat deposition values at the focus, calculated either analytically from the shock amplitude or by numerical simulation. The dependencies of the amplitude of the developed shock and peak pressures at the focus on transducer parameter F_{number} were obtained. Thus, e.g., it was shown that to generate shocks with an amplitude of about 80 MPa, transducers with $F_{numbers}$ close to unity should be used. Note that the transducers of many modern HIFU systems have geometry suitable to produce similar levels of shocks. In less-focused fields, shock fronts will form for smaller pressure levels at the focus; in more-focused fields - for larger pressure levels. Saturation effects lead to a possible increase in the shock amplitude at the focus by 60% in comparison to the amplitude of the fully developed shock, which is achieved for a threefold increase in pressure amplitude at the transducer.

Our quantitative dependencies of the amplitude of a developed shock and corresponding peak pressures in the wave profile at the focus on the F_{number} of a transducer can be used in developing novel HIFU systems for specific clinical applications, which require specific levels of shock wave action.

ACKNOWLEDGMENTS

The study was supported by Russian Science Foundation grant no. 14-12-00974.

REFERENCES

1. L. R. Gavrilov, *High Intensity Focused Ultrasound in Medicine*, (Fazis, Moscow, 2013) [in Russian].
2. T. J. Dubinsky, C. Cuevas, M. K. Dighe, O. Kolokythas, and J. H. Hwang, AJR Am. J. Roentgenol. **190**, 191 (2008).
3. M. R. Bailey, S. G. Kargl, L. A. Crum, V. A. Khokhlova, and O. A. Sapozhnikov, Acoust. Phys. **49**, 369 (2003).
4. W. J. Elias, D. Huss, T. Voss, J. Loomba, M. Khaled, E. Zadicario, R. C. Frysinger, S. A. Sperling, S. Wylie, S. J. Monteith, J. Druzgal, B. B. Shah, M. Harrison, and M. Wintermark, New England J. Med. **369**, 640 (2013).
5. E. J. Dorenberg, F. Courivaud, E. Ring, K. Hald, J. A. Jakobsen, E. Fosse, and P. K. Hol, Minim. Invasive Therapy and Allied Technol. **22**, 73 (2013).
6. F. Wu, Z. B. Wang, W. Z. Chen, J. Z. Zou, J. Bai, H. Zhu, K. Q. Li, F. L. Xie, C. B. Jin, H. B. Su, and G. W. Gao, Ultrasound Med. Biol. **30**, 245 (2004).
7. A. Maxwell, O. Sapozhnikov, M. Bailey, L. Crum, Z. Xu, B. Fowlkes, C. Cain, and V. Khokhlova, Acoustics Today **8**, 24 (2012).
8. O. V. Bessonova, V. A. Khokhlova, M. R. Bailey, M. S. Canney, and L. A. Crum, Acoust. Phys. **55**, 463 (2009).
9. E. A. Filonenko and V. A. Khokhlova, Acoust. Phys. **47**, 468 (2001).
10. M. Canney, V. Khokhlova, O. Bessonova, M. Bailey, and L. Crum, Ultrasound Med. Biol. **36**, 250 (2010).
11. J. Parsons, C. Cain, G. Abrams, and J. Fowlkes, Ultrasound Med. Biol. **32**, 115 (2006).
12. T. D. Khokhlova, M. S. Canney, V. A. Khokhlova, O. A. Sapozhnikov, L. A. Crum, and M. R. Bailey, J. Acoust. Soc. Am. **130**, 3498 (2011).
13. J. M. Keller, G. R. Schade, K. Ives, X. Cheng, T. J. Roso, M. Piert, J. Siddiqui, W. W. Roberts, and E. T. Keller, The Prostate **73**, 952 (2013).
14. M. M. Karzova, M. V. Averiyanov, O. A. Sapozhnikov, and V. A. Khokhlova, Acoust. Phys. **58**, 81 (2012).
15. E. A. Zabolotskaya and R. V. Khokhlov, Akust. Zh. **15**, 35 (1969).
16. V. P. Kuznetsov, Akust. Zh. **16**, 467 (1971).
17. C. Perez, H. Chen, T. J. Matula, M. M. Karzova, and V. A. Khokhlova, J. Acoust. Soc. Am. **134**, 1663 (2013).
18. M. S. Canney, M. R. Bailey, L. A. Crum, V. A. Khokhlova, O. A. Sapozhnikov, J. Acoust. Soc. Am. **124**, 2406 (2008).
19. O. V. Bessonova and V. Wilkens, IEEE Trans. Ultrason. Ferroelectr. Freq. Control **60**, 290 (2013).
20. O. V. Bessonova, V. A. Khokhlova, M. S. Canney, M. R. Bailey, and L. A. Crum, Acoust. Phys. **56**, 354 (2010).
21. V. A. Khokhlova, A. D. Maxwell, P. V. Yuldashev, P. B. Rosnitskiy, W. Kreider, O. A. Sapozhnikov, and M. R. Bailey, in *Proc. IEEE Int. Ultrasonics Symp.,* Chicago, 2014 p. 422.

Translated by A. Carpenter